



## H<sub>2</sub>S-driven sensitization and inhibition of CH<sub>4</sub> oxidation: An experimental and wide-range kinetic-modeling study

Alessandro Stagni<sup>a,\*</sup>, Suphaporn Arunthanayothin<sup>b</sup>, Olivier Herbinet<sup>b</sup>,  
Frédérique Battin-Leclerc<sup>b</sup>, Tiziano Faravelli<sup>a</sup>

<sup>a</sup> Department of Chemistry, Materials, and Chemical Engineering "G. Natta", Politecnico di Milano, Milano 20133, Italy

<sup>b</sup> Laboratoire Réactions et Génie des Procédés, CNRS-Université de Lorraine, 1 rue Grandville, 54000 Nancy, France

### ARTICLE INFO

#### Keywords:

Hydrogen sulfide  
Sulfur oxides  
Jet-stirred reactor  
Detailed kinetics  
Oxidation

### ABSTRACT

The recent diversification of the energy sources has brought about a renewed interest in hydrogen sulfide (H<sub>2</sub>S) chemistry and its mutual interaction with conventional fuels. In this work, the oxidation of methane (CH<sub>4</sub>) with and without the addition of 500 ppm H<sub>2</sub>S was experimentally investigated in a jet-stirred reactor, at near-atmospheric conditions (107 kPa), low temperatures (450 to 1200 K) and lean-to-rich compositions (0.5 ≤ Φ ≤ 2), with a residence time τ = 2 s. At the same time, a kinetic model was set up to shed light on the fundamental couplings between carbon and sulfur chemistry.

For all the conditions, the presence of H<sub>2</sub>S caused an earlier oxidation onset of CH<sub>4</sub> consumption, compared to the pure fuel. On the other hand, H<sub>2</sub>S consumption occurred over a wider temperature range, starting at temperatures as low as 650 K. The kinetic model was able to unravel the interactions resulting in this behavior: the two fuels were found to interact at both radical pool level (OH/O/H), as well as at fuel radical level, through mutual H-abstraction (CH<sub>3</sub>+H<sub>2</sub>S ↔ CH<sub>4</sub>+SH) and radical recombination providing methanethiol (CH<sub>3</sub>+SH ↔ CH<sub>3</sub>SH). While fuel–fuel H-abstraction was found to significantly affect only the low-temperature behavior, the importance of CH<sub>3</sub>SH chemistry was framed in a wider range of conditions. The extended model validation confirmed indeed an inhibiting effect of CH<sub>3</sub>SH in the higher-temperature flame propagation of dual-fuel mixtures, whose flame speed had been previously observed to be lower than those of pure fuels.

### 1. Introduction

The progressive integration of unconventional fuels in the energy market is resulting in new scientific and technological challenges to be overcome, in order to ensure their efficient and harmless exploitation. They also include shale gas [1], and within the undergoing energy transition, biogas, and biooils produced from the fast pyrolysis of lignocellulosic biomass [2]. In all of them, trace amounts of sulfur compounds are present, from tens to thousands of parts per million (ppm), needing proper treatment ahead of fuel utilization.

The Claus process [3] is currently the leading technology used for removing H<sub>2</sub>S by converting it into elemental sulfur. Although enhancements such as oxygen-enriched air streams have been introduced to enhance sulfur recovery and process variable H<sub>2</sub>S concentrations [4], the direct combustion of untreated gas has been recently proposed as a cost-effective alternative, with a downstream removal of Sulfur Oxides (SO<sub>x</sub>) [5,6].

Exploring such a technological pathway requires a thorough knowledge of the combustion chemistry of sulfur-containing compounds,

which are mostly present under the form of Hydrogen Sulfide (H<sub>2</sub>S) [2]. Indeed, although the lack of understanding in H<sub>2</sub>S oxidation chemistry has been partially filled in the latest years, tackling such a topic also includes unraveling the effect of H<sub>2</sub>S on the oxidation features of other hydrocarbons. As a matter of fact, the recent literature has shown that even small amounts of H<sub>2</sub>S are able to alter the reactivity of hydrogen [7], syngas [8] and methane [9–14]. Such mixtures have actually shown a complex, non-linear behavior, exhibiting effects in the opposite directions: when doping H<sub>2</sub>/O<sub>2</sub> mixtures with H<sub>2</sub>S, Mathieu et al. [7] showed an increase in the Ignition Delay Time (IDT) of H<sub>2</sub>, except at high pressures (33 atm) and low temperatures (< 1100 K), with higher amounts of H<sub>2</sub>S (1600 ppm). A comparable behavior was later observed when adding H<sub>2</sub>S impurities to syngas (H<sub>2</sub>/CO) blends [8].

Moving to CH<sub>4</sub>/H<sub>2</sub>S co-oxidation, Gersen et al. [11] showed that, at pressures between 30 and 80 bar, the addition of 1% H<sub>2</sub>S resulted in halving the IDTs of pure CH<sub>4</sub>. Still at high pressures (50 bar), when studying the oxidation of binary mixtures in a Flow Reactor (FR), they showed that H<sub>2</sub>S consumption begins much before the onset of CH<sub>4</sub>

\* Corresponding author.

E-mail address: [alessandro.stagni@polimi.it](mailto:alessandro.stagni@polimi.it) (A. Stagni).

oxidation (i.e. even before 600 K). Such effect was similarly observed by Colom-Díaz et al. [12] in FR conditions, for a wide range of pressures (0.65–40 bar) and equivalence ratios. In particular, the oxidation onset of CH<sub>4</sub> was found to occur at lower temperatures compared to the pure fuel (especially at high pressures), while H<sub>2</sub>S oxidation was delayed by the presence of CH<sub>4</sub> at atmospheric conditions. Finally, Laminar Flame Speed (LFS) experiments [14–16] showed that replacing CH<sub>4</sub> with H<sub>2</sub>S resulted in a decrease of LFS values in stoichiometric and rich conditions.

At a theoretical level, few works investigating the interaction between H<sub>2</sub>S and CH<sub>4</sub> were carried out in the last decade. They were mostly focused on the evaluation of H-abstractions by the SH radical from hydrocarbons [17] as well as by S/SO/S<sub>2</sub> [18]. As a result, even the most recent kinetic models had to include several estimations and/or rate rules, like those proposed by Van de Vijver et al. [19] for alkyl sulfide pyrolysis, later implemented in further works [14,20]. When setting up a detailed mechanism for the oxy-combustion of sour gas, Bongartz and Ghoniem [21] pointed out that even a data-driven optimization procedure was not enough to ensure a satisfactory agreement in all the literature datasets (e.g. FR, LFS). The successive kinetic modeling works were mostly performed in support of the respective experimental campaigns [11–14], and highlighted the challenges in obtain a kinetic mechanism with a sufficient degree of generality.

The mentioned experimental works highlight that the most critical region is represented by low-temperature operating conditions, where fuel–fuel interactions might play an important role in regulating the radical pool due to the slower reactivity. In this context, this work aims at framing the role of such interactions through a combined experimental and modeling approach: a novel campaign was performed in a Jet Stirred Reactor (JSR) under diluted conditions, and with variable equivalence ratios (lean to rich). To the authors' knowledge, this is the first time CH<sub>4</sub>/H<sub>2</sub>S co-oxidation was studied in a JSR facility. A comprehensive analysis of reactants, products and intermediates was carried out. At the same time, by building upon a core H<sub>2</sub>S mechanism previously set up, a kinetic mechanism describing CH<sub>4</sub>/H<sub>2</sub>S oxidation was developed. This was leveraged to gain a more comprehensive understanding of the results from the experimental device, identifying the key steps and competitions driving reactivity, and to obtain indications about future theoretical and kinetic-modeling research.

## 2. Methodology

### 2.1. Experimental setup

The oxidation of methane doped with hydrogen sulfide was experimentally investigated using a jet-stirred reactor (JSR) already described in previous works [22,23], working close to atmospheric pressure (107 kPa), and operated at steady state. The reactor consists of a spherical vessel with injection of the fresh mixture through four nozzles located at its center, creating high turbulence resulting in homogeneity in composition and temperature. As a result, the JSR can be modeled as a perfectly stirred reactor. Experiments were carried out at temperatures ranging from 450 to 1200 K and at a residence time  $\tau = 2.0$  s. The mixtures composition is reported in Table 1. Six fuel blends were considered, with and without H<sub>2</sub>S to assess its chemical role. All the fuel mixtures were composed of 2% CH<sub>4</sub> and 500 ppm H<sub>2</sub>S (where present), with helium as dilution gas. Three equivalence ratios ( $\Phi$ ) were considered (0.5, 1.0 and 2.0). The fuel-air equivalence ratio was calculated according to the two following stoichiometric equations: CH<sub>4</sub> + 2O<sub>2</sub> → 2H<sub>2</sub>O + CO<sub>2</sub>, and H<sub>2</sub>S + 1.5O<sub>2</sub> → H<sub>2</sub>O + SO<sub>2</sub>. Mass flow controllers were used for reactor feeding (relative uncertainty of ±0.5% in flow). Gases were provided by Messer (H<sub>2</sub>S at 925 ±2 ppm in helium, purities of 99.99% for helium and oxygen) and Air Liquide (CH<sub>4</sub> 99.995% pure).

The fused silica wall of the JSR was treated with a solution of boric acid (boric acid in 50% water - 50% ethanol) to form an impervious

**Table 1**  
Experimental conditions (He as balance gas).

Exp ID	CH <sub>4</sub> [-]	H <sub>2</sub> S [ppm]	O <sub>2</sub> [-]	$\Phi$ [-]
1	0.02	–	0.08	0.5
2	0.02	–	0.04	1
3	0.02	–	0.02	2
4	0.02	500	0.0815	0.5
5	0.02	500	0.04075	1
6	0.02	500	0.0204	2

layer of boric oxide to avoid undesirable catalytic effects that were observed in the present study. The occurrence of wall catalytic effects had already been observed in a previous work on H<sub>2</sub>S [24] and was also reported by others [25]. The following methodology, inspired by the literature [25], was followed to treat the wall: the tube was first filled with a saturated solution of boric acid, then it was drained and dried with helium flowing through. The tube was heated to 393 K to eliminate the remaining solvent molecules. To obtain the impervious layer covering the wall, the reactor was then time heated at 500 °C (773 K): the obtained layer was white and translucent before the heating, and became invisible after the heating, as mentioned in literature. The procedure was repeated twice as the geometry of the fused silica jet-stirred reactor is complex. Although the washing of the boric oxide layer over time cannot be excluded, no deviations in data were observed during the time of these experiments (more than one month), thus suggesting longer time scales for washing to eventually occur.

The reactants and reaction products were analyzed using two diagnostics, gas chromatography and on-line mass spectrometry: (1) a first gas chromatograph (GC) was used for the quantification of carbon-containing species such as methane, carbon monoxide, carbon dioxide and the three C<sub>2</sub> hydrocarbons (the carrier gas was helium). It was equipped with a PlotQ capillary column and included a Flame Ionization Detector (FID) preceded by a methanizer (for the reduction of oxygenated functional groups over a heated nickel catalyst) allowing a better sensitivity for CO and CO<sub>2</sub>. (2) a second gas chromatograph was used for the detection of O<sub>2</sub>. It was equipped with a Carbosphere packed column and a thermal conductivity detector. Calibrations of both gas chromatographs were performed using gaseous standards or using the “effective carbon number” method for carbon containing species [23]. Relative uncertainties in mole fractions of species detected by gas chromatography are ±5% for methane, O<sub>2</sub>, CO and CO<sub>2</sub> and ±10% for C<sub>2</sub> hydrocarbons. (3) On-line mass-spectrometry was used to detect hydrogen sulfide, sulfur dioxide, water, and hydrogen. Sampling was achieved through a capillary tube directly connecting the JSR outlet and the analyzer. This technique requires the calibration of each species as there is no obvious relationship between their structures and their calibration factors. Gaseous standards were used except for water, which was calibrated considering the reaction complete at the highest temperature. It is ±10% for calibrated species (H<sub>2</sub>S, SO<sub>2</sub>, and H<sub>2</sub>) and ±20% for water. Atom-balances were performed for C, H and S. Overall C and H balances are correct over the whole temperature range and whatever the equivalence ratio (1.02 ± 0.06 and 0.99 ± 0.04 for C and H in the mixture case, 1.02 ± 0.05 for C in the neat methane case, respectively). The S balance is also acceptable (overall 1.00 ± 0.06) with slightly more deviations under lean conditions than under stoichiometric and rich ones.

It is worth mentioning that, due to its potential importance in the experimental conditions investigated, a search for CH<sub>3</sub>SH was also performed, but it could not be observed in gas chromatography analyses, nor in mass spectrometry ones. This might be due to the loss of this species at the wall of the pipes used for transferring species from the reactor to the analytical section.

### 2.2. Kinetic modeling

The kinetic modeling of the pyrolysis and oxidation of CH<sub>4</sub>/H<sub>2</sub>S mixtures was performed through a hierarchical approach. With regard

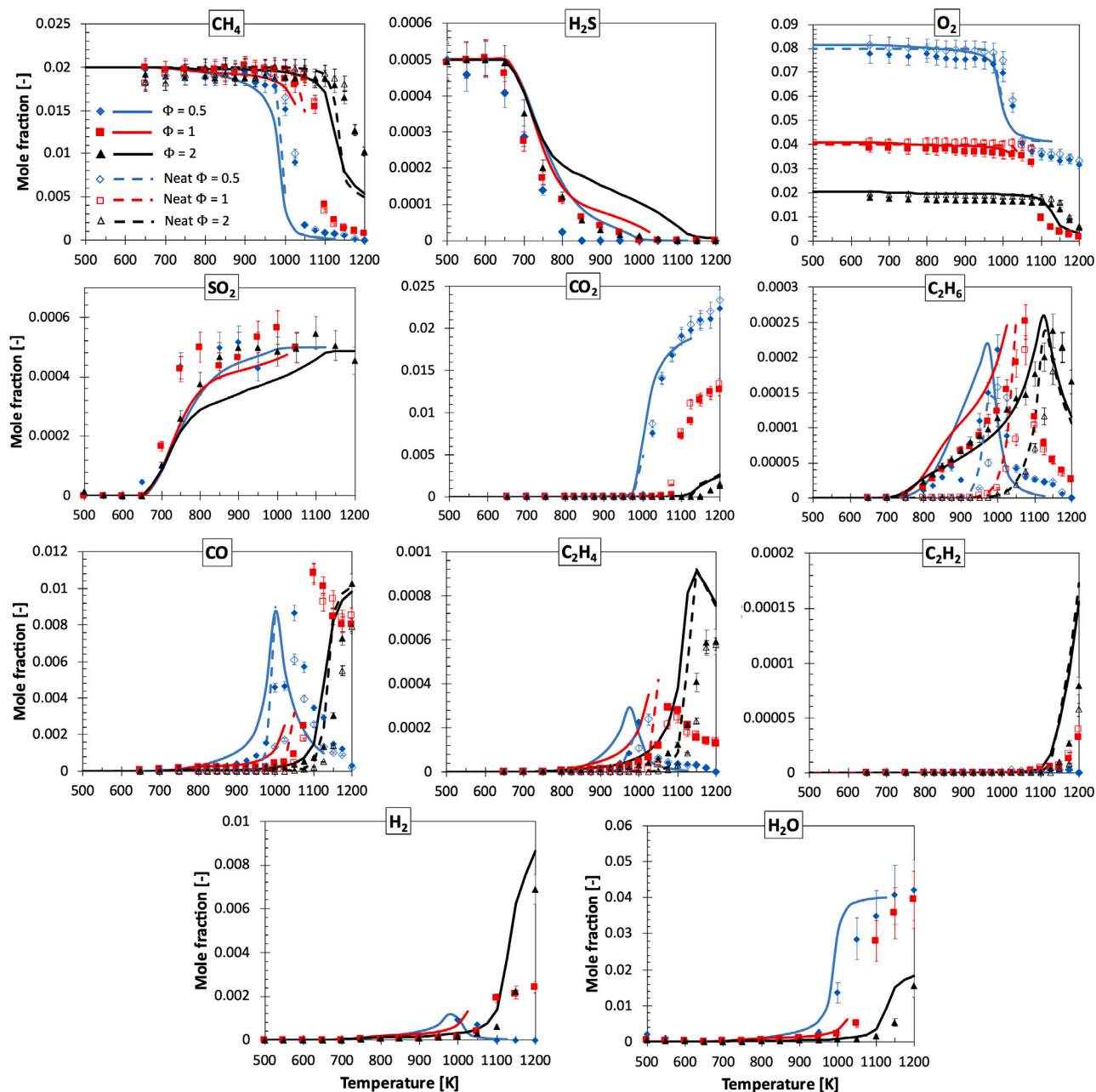


Fig. 1. Mole fractions of reactants, main reaction products and intermediates at variable  $T$  and  $\phi$  in the JSR. Symbols: experiments. Lines: data computed with the kinetic model when the steady state regime was established.

to  $\text{CH}_4$ , this was set up with a core  $\text{C}_0$ - $\text{C}_2$  module from Metcalfe et al. [26], and  $\text{C}_3$  from Burke et al. [27]. Such a core mechanism is common to the whole CRECK kinetic framework, and was shown to provide reasonably good predictions for a variety of fuels, against a wide range of experimental conditions and datasets [28]. On the other hand,  $\text{H}_2\text{S}$  sub-mechanism relied on the previous work by Stagni et al. [24] for the pure fuel, where several key reaction steps were re-evaluated through a first-principles methodology, based on an *ab initio*, transition state theory based master equation (ME) approach [29]. With regard to the C-S interactions, they were organized with a modular methodology:

- i The H-abstraction by  $\text{CH}_3$  from  $\text{H}_2\text{S}$  was taken from the database of H-abstractions evaluated *ab initio* in the recent work of Cavallotti et al. [29]. On the other hand, H-abstractions by SH from heavier hydrocarbons, and by S/SO/S $_2$  from methane were taken from the works of Zeng et al. [17,18].

- ii The sub-mechanism of the oxidation of methanethiol ( $\text{CH}_3\text{SH}$ ), present in trace amounts in biogas, but also an important intermediate in  $\text{CH}_4/\text{H}_2\text{S}$  oxidation, was taken from the recent work of Gersen et al. [11].  $\text{CH}_3\text{SH}$  decomposition reactions were updated through RMG rate rules [30].
- iii Carbon disulfide ( $\text{CS}_2$ ) and carbonyl sulfide (COS) sub-mechanisms were taken from the modeling works of Glarborg and coworkers [31,32].

Thermodynamic properties were taken from the database of Burcat and Ruscic [33] and RMG database [30]. The complete mechanism includes 141 species and 2224 reactions, and is available as Supplemental Material (SM) in CHEMKIN format, along with thermodynamic and transport properties. In order to assess its generality features, a wide-range validation against the available literature data is shown in the SM, too.

### 3. Results and discussion

#### 3.1. Experimental results

Considering the compositions listed in Table 1, Fig. 1 shows the experimental profiles of fuel, oxidizer and main reaction products, as well as their related kinetic modeling predictions. It is important to highlight that simulation results are shown only when steady-state conditions are attained. In lean and stoichiometric conditions, after the onset of CH<sub>4</sub> oxidation, a dynamic behavior, i.e. an oscillating combustion with repeated extinctions and ignitions, was often observed: this is a well-known phenomenon in well-stirred reactors [22], whose chemical roots had been previously investigated [34,35]. Yet, in the present work, the oscillating behavior was predicted by the model but not observed experimentally: indeed, oscillations are highly sensitive to the kinetic rates of the termination reactions, thus the range of temperatures where they occur might not always be caught.

When analyzing the experimental and predicted consumption trends of the two fuels, two important observations can be made. First of all, in spite of the small amounts (500 ppm), the addition of H<sub>2</sub>S to CH<sub>4</sub> causes an anticipation of CH<sub>4</sub> oxidation onset at all the  $\Phi$  values. This is not immediate to be identified through the experimental points, due to their resolution (25 K) and their uncertainty ( $\pm 10\%$ ). Such a difference is instead easier to be quantified through model predictions: considering 10% conversion of CH<sub>4</sub> as a reference, the predicted onset is anticipated by 40 to 75 K, with higher values under lean conditions. Apparently, the addition of H<sub>2</sub>S slows down the conversion rate of CH<sub>4</sub>, occurring over a wider temperature range, instead of the usual abrupt consumption observed with the pure fuel, observed in this work as well as in previous ones [22]. For all the datasets, the kinetic model is able to reproduce the experimental trends of CH<sub>4</sub>, reaction products and C<sub>2</sub> intermediates reasonably well. A slightly early onset ( $\sim 30$  K) in the oxidation is predicted in both pure CH<sub>4</sub> and CH<sub>4</sub>/H<sub>2</sub>S mixtures, which can be observed for intermediate products, too. Apart from that, the shape of the curves is reproduced very well for all the species.

The second point to be raised is the earlier oxidation of H<sub>2</sub>S compared to CH<sub>4</sub>. All the H<sub>2</sub>S profiles share a common inception temperature at 650 K, regardless of  $\Phi$  value. In leaner conditions ( $\Phi = 0.5$ ) a small conversion ( $\sim 20\%$ ) is measured when transitioning from 500 K to 700 K. As already previously observed with pure H<sub>2</sub>S [24], this might be due to residual wall effects, persisting after the treatment described in Section 2.1. However, the temperature at which H<sub>2</sub>S reaches 50% conversion ( $T_{50\%}$ ) is comparable for the 3 cases. The kinetic model is able to predict both the inception temperature for  $\Phi = 1$  and 2, and  $T_{50\%}$  for H<sub>2</sub>S for all the datasets reasonably well, and the same holds for SO<sub>2</sub> trends. The H<sub>2</sub>S conversion rate through the temperature range is also well predicted, except at  $\Phi = 2$ , where the model predicts a slower conversion rate at higher temperatures, differently from what experimentally detected. However, with the current mechanism there is no way to explain this deviation, at the same time retaining the physical meaning of the reaction rates and the predictive features of the mechanism (i.e. in a wider range of operating conditions, as shown in the SM).

It is very interesting to notice that this is not the first time that such effects were experimentally observed for CH<sub>4</sub>/H<sub>2</sub>S mixtures: in their work, Colom-Díaz et al. [12] showed that, in two different FR configurations, the presence of H<sub>2</sub>S caused an anticipation in the onset of CH<sub>4</sub> oxidation, too, at atmospheric as well as high-pressure conditions, although occurring, in the pure-fuel case, at much higher temperatures ( $\geq 1300$  K). Similarly, at atmospheric pressure, H<sub>2</sub>S consumption in the presence of CH<sub>4</sub> was distributed over a wider range of temperatures, compared to the pure-fuel case. On the other hand, the onset of H<sub>2</sub>S oxidation always occurred at similar temperatures as the pure-fuel case, as can be noticed also by comparing the present results with the previous work by Stagni et al. [24] under lean conditions.

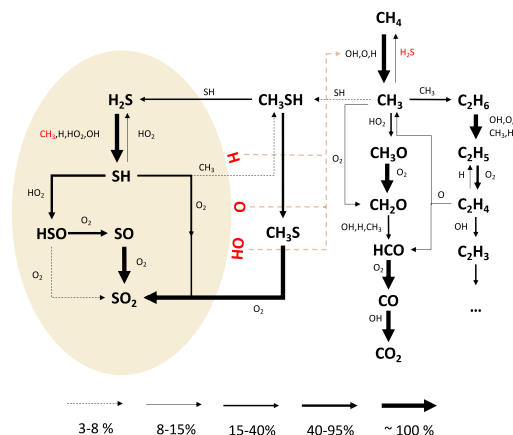


Fig. 2. Carbon and sulfur flux analysis, respectively, in the oxidation of 500 ppm H<sub>2</sub>S and 2% CH<sub>4</sub> in JSR ( $T = 900$  K -  $\Phi = 0.5$ ). Flux intensity is related to the single molecule.

#### 3.2. Kinetic analysis

In order to unravel the couplings between the two fuels, flux analysis was carried out for sample conditions, i.e. at the onset of CH<sub>4</sub> oxidation ( $\sim 10\%$  conversion) at  $\Phi = 0.5$  (Fig. 2).

Qualitatively, both CH<sub>4</sub> and H<sub>2</sub>S follow the conversion paths, which can be observed for the pure fuels at such relatively low temperatures [22,24]. The coupling, and thus the mutual interaction, occurs at three different levels: (i) first of all, the oxidation process of H<sub>2</sub>S, starting in pure conditions at temperatures much lower than CH<sub>4</sub> (700 K vs at least 1000 K) and converting the fuel to SO<sub>2</sub>, acts as a pool of OH, O and H radicals. As a result, they become available for H-abstraction from CH<sub>4</sub>, thus forming CH<sub>3</sub> and triggering its parallel oxidation. (ii) At the same time, the second interaction is generated by the mutual H-abstraction ( $\text{CH}_3 + \text{H}_2\text{S} \rightarrow \text{CH}_4 + \text{SH}$ ): indeed, the formation of CH<sub>3</sub> through the dynamics just described enables a further H-abstraction by the same radical, from H<sub>2</sub>S itself. This further boosts the oxidation of H<sub>2</sub>S, contributing to an earlier conversion. (iii) Third, the process is slowed down by the formation of CH<sub>3</sub>SH through CH<sub>3</sub> and SH recombination (written as a decomposition reaction in the current mechanism), which subtracts SH radicals from H<sub>2</sub>S oxidation path.

Such couplings find further support in Fig. 3a, showing the reactions driving CH<sub>4</sub> oxidation for variable  $\Phi$ . In addition to the well-known competitions in the low-temperature oxidation of methane for consuming CH<sub>3</sub> radicals, the SH+HO<sub>2</sub> channel (propagation via HSO+OH vs termination to H<sub>2</sub>S+O<sub>2</sub>) regulates the reactivity of methane, too, as it sets the radical pool. On the other hand, the recombination of CH<sub>3</sub> and SH inhibits the process, as already said, with an increasing importance at stoichiometric and rich  $\Phi$ .

This mechanism explains the delayed consumption of H<sub>2</sub>S in the presence of CH<sub>4</sub>, and is confirmed in the sensitivity analysis to H<sub>2</sub>S mass fraction reported in Fig. 3b at its half-conversion temperature (750 K), common for all the  $\Phi$  values. In addition to the key reaction steps driving H<sub>2</sub>S combustion, CH<sub>3</sub> self-recombination and recombination with SH slow down the oxidation process, as they both subtract active radicals from the fuel-fuel H-abstraction, which instead enhances oxidation.

It is also worth highlighting that CH<sub>3</sub>O<sub>2</sub> and CH<sub>3</sub>O were both shown playing a critical role in the low-temperature oxidation of CH<sub>4</sub>. Recently, possible interactions with sulfur-containing species were assessed in literature by Zhang et al. [36], although no full rate constants are provided (thus were not included in the model). In the next future, the inclusion of such reaction pathways in the current model might shed light on their actual importance in the investigated conditions.



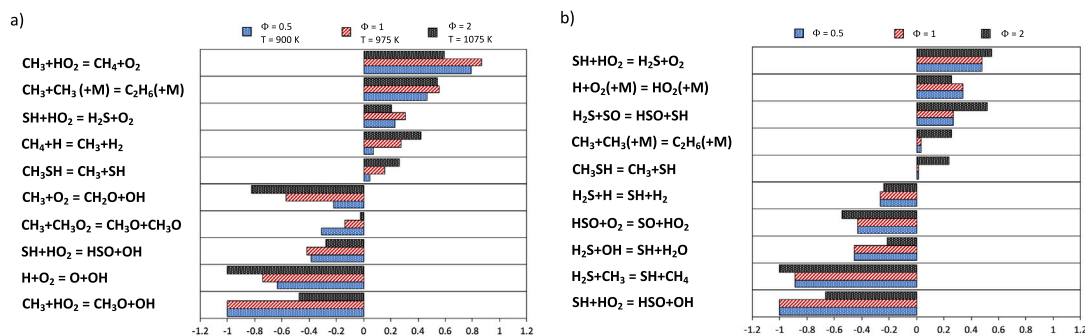


Fig. 3. Sensitivity coefficients to (a)  $\text{CH}_4$  mass fraction in the oxidation of 500 ppm  $\text{H}_2\text{S}$  and 2% $\text{CH}_4$  in JSR, at  $\sim 10\%$   $\text{CH}_4$  conversion, and (b)  $\text{H}_2\text{S}$  mass fraction in the oxidation of 500 ppm  $\text{H}_2\text{S}$  and 2% $\text{CH}_4$  in JSR ( $T = 750$  K).

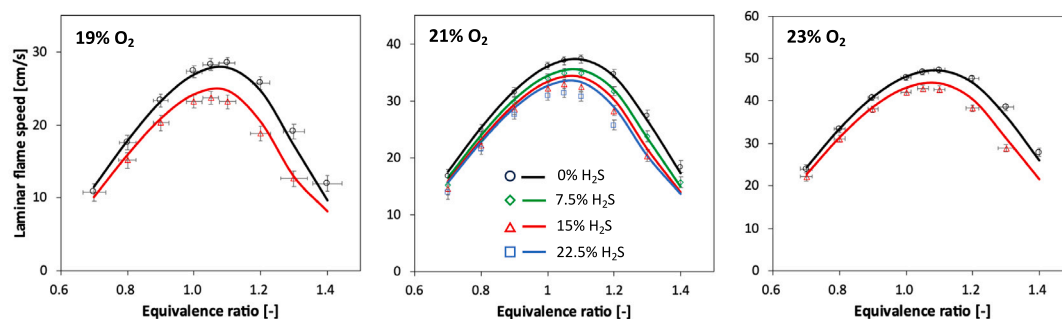


Fig. 4. Laminar flame speed of  $\text{CH}_4/\text{H}_2\text{S}/\text{O}_2/\text{N}_2$  mixtures ( $P = 1$  atm -  $T_u = 298$  K). Experimental data [15,16] and modeling predictions.

### 3.3. Carbon–sulfur interaction

The analysis of the reaction pathways involved in the low-temperature oxidation of  $\text{CH}_4/\text{H}_2\text{S}$  pointed out that carbon–sulfur interaction occurs indirectly at a radical pool level as well as directly at a fuel radical level. In order to assess the generality of the kinetic framework as well as to obtain general conclusions to address future activity, their combined effect was further investigated in flame propagation conditions. As pure fuels,  $\text{H}_2\text{S}$  flames propagate faster than  $\text{CH}_4$  ones. Yet, recent experimental works [14–16] have highlighted the slower flame speeds of  $\text{CH}_4$  blends with small amounts of  $\text{H}_2\text{S}$ . The role of carbon–sulfur interaction in flame propagation was then unraveled through a comprehensive analysis of  $\text{CH}_4/\text{H}_2\text{S}/\text{O}_2/\text{N}_2$  flames, on the wake of what experimentally done by Han et al. [15,16]. Fig. 4 reports the experimental measurements at ambient conditions, and the related predictions obtained through the developed kinetic mechanism, for variable  $\text{O}_2$  mole fraction and  $\text{H}_2\text{S}$  amount in the fuel blend.

For all the  $\text{O}_2$  amounts, the modeling predictions confirm the experimental trends with a reasonable accuracy and a slight overestimation for the highest amounts of  $\text{H}_2\text{S}$ . A progressive reduction of the flame speed value with the addition of  $\text{H}_2\text{S}$  is observed, although such decrease tends to flattening, and a maximum inhibiting effect with a successive increase of LFS is expected to be reached for further  $\text{H}_2\text{S}$  additions. This is opposite with respect to what observed in the JSR case: in order to untangle this, sensitivity analysis was performed, and sensitivity coefficients with respect to H mass fraction were calculated in correspondence of the flame front, anchored at the center of the computational grid. For the sake of compactness, Fig. 5 shows only the reactions involving C–S interaction are shown, in addition to a subset of most relevant  $\text{CH}_4$ -related reactions used as reference values.

In addition to the  $\text{CH}_3$  termination to  $\text{CH}_4$ , a key role is played by its recombination to  $\text{CH}_3\text{SH}$ . As in the low-temperature conditions, this step inhibits the reactivity by absorbing reactive SH radicals. Because

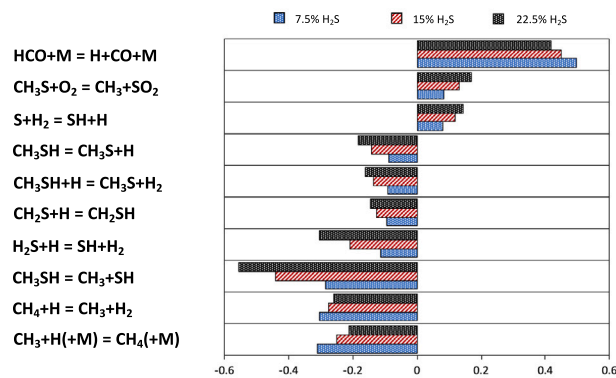


Fig. 5. Sensitivity coefficients of the most relevant reactions to H mass fraction in the laminar flame propagation of  $\text{CH}_4/\text{H}_2\text{S}/\text{O}_2/\text{N}_2$  mixtures ( $P = 1$  atm -  $T_u = 298$  K -  $\phi = 1$ ), normalized with respect to the value of  $\text{H} + \text{O}_2 \rightarrow \text{O} + \text{OH}$ .

of this, they are taken away from the branching path  $\text{SH} + \text{O} \rightarrow \text{SO} + \text{H}$ , which combined with the successive step  $\text{SO} + \text{O}_2 \rightarrow \text{SO}_2 + \text{O}$ , results in a net  $\text{SH} + \text{O}_2 \rightarrow \text{SO}_2 + \text{H}$ , i.e. providing the more reactive H radicals. Above all, Fig. 5 shows that the whole  $\text{CH}_3\text{SH}$  chemistry is actually of primary importance for the overall inhibiting effect: the H-abstraction by the H radical from  $\text{CH}_3\text{SH}$  further decreases the overall reactivity as it consumes reactive H atoms returning less reactive methylthio radical ( $\text{CH}_3\text{S}$ ). On turn, the competition between  $\text{CH}_3\text{S}$  oxidation and termination provides a further contribution to set the overall reactivity.

Considering the whole  $\text{CH}_4/\text{H}_2\text{S}$  oxidation mechanism,  $\text{CH}_3\text{SH}$  chemistry represents the most critical subset: several of its related rates are indeed based on estimations, and a systematic and high-level theoretical activity has been mostly focused on the related H-abstractions by

the major radicals. In particular, there is a substantial lack of fundamental knowledge on the dissociation reactions (or related recombinations, in the reverse direction) involving  $\text{CH}_3\text{SH}$ , providing  $\text{CH}_3+\text{SH}$ , as well as  $\text{CH}_3\text{S}+\text{H}$  and  $\text{CH}_2\text{SH}+\text{H}$ . The importance of  $\text{CH}_3\text{SH}$  dissociation both in jet-stirred and flame propagation conditions calls for an accurate temperature dependency for all of the three rates. Moreover, as already pointed out by Van de Vijver et al. [19], it is possible that such recombinations might be in the fall-off regime, rather than in the high-pressure limit. Nevertheless, the available literature rates [19,37], as well as those adopted in this work [30], do not account for the pressure effect. As a matter of fact, high-pressure experiments [11–13] have often shown the largest disagreements with kinetic models. Therefore, fundamental studies framing such a role are desirable for a further improvement and generalization of the kinetic model.

#### 4. Conclusions

In this work, the complex chemical role of hydrogen sulfide in the co-oxidation with methane was investigated through a combined experimental and kinetic modeling methodology. In order to investigate the most kinetically critical (and least explored) conditions where such interactions are established, experiments were performed in a JSR, at low temperatures (450 to 1200 K) and lean-to-rich (0.5 to 2) equivalence ratios. Initial conditions with and without 500 ppm  $\text{H}_2\text{S}$  were considered, in order to assess the net effect of its addition. In parallel, a kinetic model was set up by relying upon previously validated  $\text{CH}_4$  and  $\text{H}_2\text{S}$  core chemistry, and including carbon–sulfur interactions, established through mutual H-abstraction, a methanethiol sub-mechanism and carbon sulfides chemistry.

The obtained experimental data showed an anticipated onset of  $\text{CH}_4$  oxidation due to the addition of  $\text{H}_2\text{S}$  for all of the investigated conditions. On the other hand, the consumption of  $\text{H}_2\text{S}$  was observed to begin at much lower temperatures (650 K), regardless of the equivalence ratio, yet with a much slower conversion rate with respect to the pure fuel [24].

The kinetic mechanism was able to reproduce the experimental trends for all the species reasonably well, especially under lean and stoichiometric conditions, with an underprediction of  $\text{H}_2\text{S}$  conversion in rich condition and higher temperatures. It provided an insight on the kinetic foundations behind the observed behavior. The higher reactivity of  $\text{H}_2\text{S}$  generates a radical pool (OH, O, H) available for H-abstraction from  $\text{CH}_4$  and anticipating its conversion. On the other hand, the  $\text{H}_2\text{S}$  consumption rate was found to be affected by the H-abstraction by  $\text{CH}_3$  from the fuel itself, enhancing its oxidation, and negatively by  $\text{CH}_3$  termination to  $\text{CH}_3\text{SH}$ , inhibiting the conversion of both fuels.

On the other hand, the sensitizing effect of  $\text{H}_2\text{S}$  on  $\text{CH}_4$  oxidation turned into an inhibiting one when considering flame propagation features of the related mixtures. In this case, the whole chemistry of  $\text{CH}_3\text{SH}$  and its decomposition products was found to be crucial, i.e. not limited to its decomposition into  $\text{CH}_3$  and  $\text{SH}$ . As a matter of fact, in spite of its importance in the whole temperature range, this is the most uncertain part from a kinetic point of view, requesting further theoretical focus in the next future to provide a comprehensive fundamental description and consolidating the predictive features of the mechanism.

#### Novelty and Significance Statement

This manuscript fills an important knowledge gap in the low-temperature interaction between hydrogen sulfide ( $\text{H}_2\text{S}$ ) and methane ( $\text{CH}_4$ ), which has not been experimentally addressed in Jet Stirred Reactors so far. From an applicative point of view, this is of crucial significance to get a comprehensive understanding of sour gas and biogas oxidation, which are occupying an increasing share of the energy portfolio. Moreover, this work provides an important step forward towards the development of a kinetic model for  $\text{CH}_4/\text{H}_2\text{S}$  oxidation

with generality features, i.e. predictive in the whole range of operating conditions, thoroughly describing sensitizing and inhibiting effects of  $\text{H}_2\text{S}$  (not limited to the present dataset, but also extended to different reactors and operating conditions).

#### CRedit authorship contribution statement

**Alessandro Stagni:** Contributed to design the research, Developed the kinetic model, Wrote the manuscript. **Suphaporn Arunthanayothin:** Performed the experiments, Revised the manuscript. **Olivier Herbinet:** Designed the experiments, Revised the manuscript. **Frédérique Battin-Leclerc:** Designed the research, Supervised the experimental campaign, Revised the manuscript. **Tiziano Faravelli:** Contributed to model development and design of experiments, Revised the manuscript.

#### Declaration of competing interest

The authors declare that they have no known competing financial interests or personal relationships that could have appeared to influence the work reported in this paper.

#### Acknowledgments

This work has been carried out under the financial support of the IMPROOF project (H2020-IND-CE-2016-17/H2020-SPIRE-S016) within the European Union Horizon 2020 research and innovation program (grant agreement no. 723706). The authors are also grateful to the COST Action CA22151 - Cyber-Physical systems and digital twins for the decarbonization of energy-intensive industries (CYPHER) for the fruitful discussions.

#### Appendix A. Supplementary data

Supplementary material related to this article can be found online at <https://doi.org/10.1016/j.proci.2024.105585>.

#### References

- [1] A. Ghazwani, R. Littke, G. Gaus, C. Hartkopf-Fröder, Assessment of unconventional shale gas potential of organic-rich mississippian and lower pennsylvanian sediments in western Germany, *Int. J. Coal Geol.* 198 (2018) 29–47.
- [2] M. Auersvald, L. Kejla, A. Eschenbacher, H.D. Thi, K.M. Van Geem, P. Šimáček, Detailed characterization of sulfur compounds in fast pyrolysis bio-oils using GC×GC-SCD and GC-MS, *J. Anal. Appl. Pyrolysis* 159 (2021) 105288.
- [3] J. Zaman, A. Chakma, Production of hydrogen and sulfur from hydrogen sulfide, *Fuel Process. Technol.* 41 (2) (1995) 159–198.
- [4] A. Gupta, S. Ibrahim, A. Al Shoaibi, Advances in sulfur chemistry for treatment of acid gases, *Prog. Energy Combust. Sci.* 54 (2016) 65–92.
- [5] N. Chakroun, A. Ghoniem, Techno-economic assessment of sour gas oxy-combustion water cycles for CO<sub>2</sub> capture, *Int. J. Greenh. Gas Control* 36 (2015) 1–12.
- [6] N. Chakroun, A. Ghoniem, High-efficiency low LCOE combined cycles for sour gas oxy-combustion with CO<sub>2</sub> capture, *Int. J. Greenh. Gas Control* 41 (2015) 163–173.
- [7] O. Mathieu, F. Deguillaume, E.L. Petersen, Effects of H<sub>2</sub>S addition on hydrogen ignition behind reflected shock waves: Experiments and modeling, *Combust. Flame* 161 (1) (2014) 23–36.
- [8] O. Mathieu, J. Hargis, A. Camou, C. Mulvihill, E. Petersen, Ignition delay time measurements behind reflected shock-waves for a representative coal-derived syngas with and without NH<sub>3</sub> and H<sub>2</sub>S impurities, *Proc. Combust. Inst.* 35 (3) (2015) 3143–3150.
- [9] D. Bongartz, S.J. Shanbhogue, A.F. Ghoniem, Formation and control of sulfur oxides in sour gas oxy-combustion: prediction using a reactor network model, *Energy Fuels* 29 (11) (2015) 7670–7680.
- [10] D. Bongartz, A.F. Ghoniem, Impact of sour gas composition on ignition delay and burning velocity in air and oxy-fuel combustion, *Combust. Flame* 162 (7) (2015) 2749–2757.
- [11] S. Gersen, M. van Essen, H. Darneveil, H. Hashemi, C.T. Rasmussen, J.M. Christensen, P. Glarborg, H. Levinsky, Experimental and modeling investigation of the effect of H<sub>2</sub>S addition to methane on the ignition and oxidation at high pressures, *Energy Fuels* 31 (3) (2017) 2175–2182.

- [12] J. Colom-Díaz, M. Lecinena, A. Peláez, M. Abián, Á. Millera, R. Bilbao, M. Alzueta, Study of the conversion of CH<sub>4</sub>/H<sub>2</sub>S mixtures at different pressures, *Fuel* 262 (2020) 116484.
- [13] J. Colom-Díaz, Á. Millera, R. Bilbao, M. Alzueta, New results of H<sub>2</sub>S oxidation at high pressures. Experiments and kinetic modeling, *Fuel* 285 (2021) 119261.
- [14] C.R. Mulvihill, C.L. Keesee, T. Sikes, R.S. Teixeira, O. Mathieu, E.L. Petersen, Ignition delay times, laminar flame speeds, and species time-histories in the H<sub>2</sub>S/CH<sub>4</sub> system at atmospheric pressure, *Proc. Combust. Inst.* 37 (1) (2019) 735–742.
- [15] X. Han, Z. Wang, Y. He, Y. Zhu, A.A. Konnov, Experimental and kinetic modeling study of the CH<sub>4</sub>+ H<sub>2</sub>S+ air laminar burning velocities at atmospheric pressure, *Combust. Flame* 244 (2022) 112288.
- [16] X. Han, R. Zhu, Y. He, Y. Zhu, Z. Wang, Experimental and kinetic study on the laminar burning velocities of CH<sub>4</sub>+ H<sub>2</sub>S+ N<sub>2</sub>+ O<sub>2</sub> flames at atmospheric pressure, *Fuel* 358 (2024) 130366.
- [17] Z. Zeng, M. Altarawneh, I. Oluwoye, P. Glarborg, B.Z. Dlugogorski, Inhibition and promotion of pyrolysis by hydrogen sulfide (H<sub>2</sub>S) and sulfanyl radical (SH), *J. Phys. Chem. A* 120 (45) (2016) 8941–8948.
- [18] Z. Zeng, B.Z. Dlugogorski, I. Oluwoye, M. Altarawneh, Co-oxidation of methane (CH<sub>4</sub>) and carbon disulfide (CS<sub>2</sub>), *Proc. Combust. Inst.* 37 (1) (2019) 677–685.
- [19] R. Van de Vijver, N.M. Vandewiele, A.G. Vandeputte, K.M. Van Geem, M.-F. Reyniers, W.H. Green, G.B. Marin, Rule-based ab initio kinetic model for alkyl sulfide pyrolysis, *Chem. Eng. J.* 278 (2015) 385–393.
- [20] M.U. Alzueta, R. Pernia, M. Abian, A. Millera, R. Bilbao, CH<sub>3</sub>SH conversion in a tubular flow reactor. Experiments and kinetic modelling, *Combust. Flame* 203 (2019) 23–30.
- [21] D. Bongartz, A.F. Ghoniem, Chemical kinetics mechanism for oxy-fuel combustion of mixtures of hydrogen sulfide and methane, *Combust. Flame* 162 (3) (2015) 544–553.
- [22] Y. Song, L. Marrodán, N. Vin, O. Herbinet, E. Assaf, C. Fittschen, A. Stagni, T. Faravelli, M.U. Alzueta, F. Battin-Leclerc, The sensitizing effects of NO<sub>2</sub> and NO on methane low temperature oxidation in a jet stirred reactor, *Proc. Combust. Inst.* 37 (1) (2019) 667–675.
- [23] M. Pelucchi, S. Namysl, E. Ranzi, A. Frassoldati, O. Herbinet, F. Battin-Leclerc, T. Faravelli, An experimental and kinetic modelling study of n-c4c6 aldehydes oxidation in a jet-stirred reactor, *Proc. Combust. Inst.* 37 (1) (2019) 389–397.
- [24] A. Stagni, S. Arunthanayothin, L.P. Maffei, O. Herbinet, F. Battin-Leclerc, T. Faravelli, An experimental, theoretical and kinetic-modeling study of hydrogen sulfide pyrolysis and oxidation, *Chem. Eng. J.* 446 (2022) 136723.
- [25] C.R. Zhou, K. Sendt, B.S. Haynes, Experimental and kinetic modelling study of H<sub>2</sub>S oxidation, *Proc. Combust. Inst.* 34 (1) (2013) 625–632.
- [26] W.K. Metcalfe, S.M. Burke, S.S. Ahmed, H.J. Curran, A hierarchical and comparative kinetic modeling study of C1- C2 hydrocarbon and oxygenated fuels, *Int. J. Chem. Kinet.* 45 (10) (2013) 638–675.
- [27] S.M. Burke, U. Burke, R. Mc Donagh, O. Mathieu, I. Osorio, C. Keesee, A. Morones, E.L. Petersen, W. Wang, T.A. DeVerter, et al., An experimental and modeling study of propene oxidation. Part 2: Ignition delay time and flame speed measurements, *Combust. Flame* 162 (2) (2015) 296–314.
- [28] G. Bagheri, E. Ranzi, M. Pelucchi, A. Parente, A. Frassoldati, T. Faravelli, Comprehensive kinetic study of combustion technologies for low environmental impact: MILD and OXY-fuel combustion of methane, *Combust. Flame* 212 (2020) 142–155.
- [29] C. Cavallotti, M. Pelucchi, Y. Georgievskii, S. Klippenstein, Estoktp: electronic structure to temperature-and pressure-dependent rate constants—a code for automatically predicting the thermal kinetics of reactions, *J. Chem. Theory Comput.* 15 (2) (2018) 1122–1145.
- [30] M.S. Johnson, X. Dong, A. Grinberg Dana, Y. Chung, D. Farina Jr., R.J. Gillis, M. Liu, N.W. Yee, K. Blondal, E. Mazeau, et al., RMG database for chemical property prediction, *J. Chem. Inf. Model.* 62 (20) (2022) 4906–4915.
- [31] P. Glarborg, B. Halaburt, P. Marshall, A. Guillory, J. Troe, M. Thellefsen, K. Christensen, Oxidation of reduced sulfur species: carbon disulfide, *J. Phys. Chem. A* 118 (34) (2014) 6798–6809.
- [32] P. Glarborg, P. Marshall, Oxidation of reduced sulfur species: carbonyl sulfide, *Int. J. Chem. Kinet.* 45 (7) (2013) 429–439.
- [33] A. Burcat, B. Ruscic, Third Millennium Ideal Gas and Condensed Phase Thermochemical Database for Combustion (With Update from Active Thermochemical Tables), Tech. rep., Argonne National Lab.(ANL), Argonne, IL (United States), 2005.
- [34] M. Lubrano Lavadera, Y. Song, P. Sabia, O. Herbinet, M. Pelucchi, A. Stagni, T. Faravelli, F. Battin-Leclerc, M. De Joannon, Oscillatory behavior in methane combustion: influence of the operating parameters, *Energy Fuels* 32 (10) (2018) 10088–10099.
- [35] A. Stagni, Y. Song, L.A. Vandewalle, K.M. Van Geem, G.B. Marin, O. Herbinet, F. Battin-Leclerc, T. Faravelli, The role of chemistry in the oscillating combustion of hydrocarbons: An experimental and theoretical study, *Chem. Eng. J.* 385 (2020) 123401.
- [36] S. Zhang, Y. Zhang, Y. Zhang, Z. Feng, C. Wang, H. Bian, J. Chen, A density functional theory study on the atmospheric reaction of CH<sub>3</sub>O<sub>2</sub> with HS: Mechanism and kinetics, *Int. J. Quantum Chem.* 120 (17) (2020) e26330.
- [37] L.G. Shum, S.W. Benson, The pyrolysis of dimethyl sulfide, kinetics and mechanism, *Int. J. Chem. Kinet.* 17 (7) (1985) 749–761.